Mössbauer Absorption Spectra of ^{119}Sn in Single Crystals of $(CH_3)_2SnF_2$ and $(CH_3)_2SnCl_2$

Hisao NEGITA, Ryukei BOKU, Makoto NAKAMURA, and Sumio ICHIBA

Department of Chemistry, Faculty of Science, Hiroshima University, Higashisenda-machi, Hiroshima 730

(Received September 2, 1976)

The Mössbauer absorption spectra of ^{119}Sn in single crystals of $(CH_3)_2SnF_2$ and $(CH_3)_2SnCl_2$ have been studied as a function of the orientation angles of the incident unpolarized gamma-ray beam with respect to the crystal axes, taking the absorber thickness effect into account. The analysis of the intensity ratios of the quadrupole splitting doublet yields the asymmetry parameter (η) and the orientation of the principal axes of the electric-field gradient with respect to the crystal axes. The value of η in $(CH_3)_2SnCl_2$ at 135 K was about 0.4, less than the value published previously. The sign of the ^{119}Sn quadrupole coupling constant (e^2qQ) in these compounds was found to be positive, as has been reported before.

Several parameters, such as the electric-field gradient (EFG) and the mean square-displacement (MSD) tensors at the sites of the resonant nuclei, can be obtained by means of the Mössbauer absorption spectra of the single-crystal samples.

Zory has discussed the analysis of the EFG in a single-crystal absorber containing ^{57}Fe and has applied his analysis to $FeCl_2 \cdot 4H_2O$ and evaluated all the EFG parameters.[1] This method has been successfully employed for the complete determination of all the parameters of the EFG tensor in the iron compounds, $Na_2[Fe(CN)_5NO] \cdot 2H_2O$,[2] $FeSO_4 \cdot 7H_2O$,[3] $FeSO_4 \cdot (NH_4)_2SO_4 \cdot 6H_2O$,[3] *etc.*[4-6]

In these cases, the analysis of the quadrupole hyperfine anisotropy, however, was based on the thin absorber approximation. Unless the absorber is extremely thin, the analysis is complicated by the partial saturation of the absorption intensity in a polarized single crystal.

The general theory of polarization effects given by Housley *et al.*[7] has been developed recently by Gibb,[8] who treated the data of the $FeSO_4 \cdot (NH_4)_2SO_4 \cdot 6H_2O$ single crystal with polarization in the absorption cross section and obtained good results.

So far no Mössbauer experiments with single crystals containing tin have been performed except for $Fe\{(\pi\text{-}C_5H_5)(CO)_2\}_2SnCl_2$,[9] with which the EFG tensor at tin has been evaluated and discussed by the use of a point-charge model. Therefore, in this paper we wish to report the results for Mössbauer absorption spectra by taking into account the absorber thickness effect in single crystals of $(CH_3)_2SnF_2$ and $(CH_3)_2SnCl_2$.

Experimental

A single crystal of $(CH_3)_2SnF_2$ was grown by the slow evaporation of its HF solution. A thin crystal plate of approximately 0.4×0.4 cm^2 could be obtained over about 8 weeks. The crystal habit has been described in detail.[10] An unusual feature is the dominance of the 001 plane, whose edges coincide with the crystallographic a direction. $(CH_3)_2SnF_2$ is a tetragonal crystal in the space group I4/mmm, with cell dimensions of $a=b=4.24$ Å and $c=14.16$ Å.[11] A unit cell contains two Sn atoms at the 2a positions (0, 0, 0) and (1/2, 1/2, 1/2), with a point symmetry of 4/mmm. The tin atoms are octahedrally surrounded by two methyl groups and four bridging fluorine atoms. These octahedra have the same orientation relative to the crystal axes. The local environment of the tin is shown in Fig. 1(a).

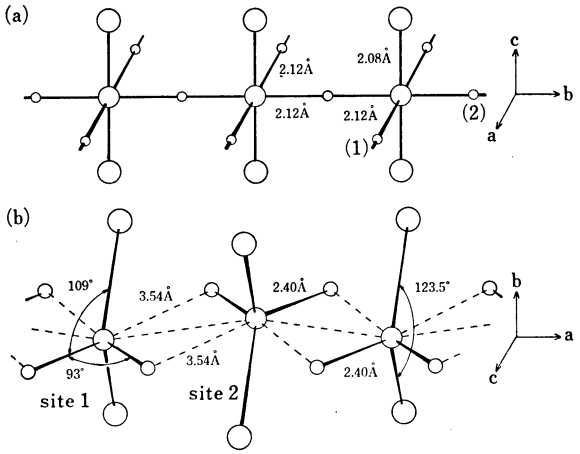

Fig. 1. The structure of (a) $(CH_3)_2SnF_2$ and (b) $(CH_3)_2SnCl_2$.
○: Me, ○: Sn, ○: Cl, and ○: F.

A large crystal of $(CH_3)_2SnCl_2$ was grown by the Bridgman method.[12] After it had been cut with a knife along the habit plane (011 and 01$\bar{1}$), we obtained a thin plate of approximately 0.7×0.7 cm^2 by the hand-polishing technique. $(CH_3)_2SnCl_2$ crystallizes in the orthorhombic space group of Imma, with unit cell dimensions of $a=8.78$, $b=7.75$, and $c=9.25$ Å.[13] The structure consists of a chain of molecules running parallel to the a axis, with the tin atoms in the distorted octahedrals. The tin and chlorine atoms in each chain are coplanar, and the methyl groups are not collinear with the tin atoms joined to their own neighbors by two bridging chlorine atoms (Fig. 1(b)).

The thickness of the crystal samples was determined by means of their weights and areas. The values of $(CH_3)_2SnF_2$ and $(CH_3)_2SnCl_2$ were 29 and 18 mg/cm^2 respectively for Sn. The crystal was mounted on a goniometer head, and the crystal axes were located by the X-ray diffraction method. Then the goniometer head was placed in a liquid nitrogen cryostat so the gamma ray might be incident perpendicularly to the crystal plate. The angle of the plate to the gamma ray was varied by the rotation of the goniometer head.

The Mössbauer spectra were obtained by the use of a constant-acceleration-type spectrometer. The gamma-ray source was 0.7 mCi ^{119}Sn in the barium stannate matrix and was used at room temperature. The absorber temperatures were 135 K for single-crystal samples and 100 K for powder. X-Rays from the source were shut out by a palladium foil 50 micron thick. The velocity scale was calibrated by the use of reference absorbers of $BaSnO_3$ and Sn foil. All the

spectra were analyzed by means of a least-squares computer fitting the Lorentzian-line shapes without constraints on the line positions, widths, and intensities by the use of HUC-III, HITAC-8700.

Method of Calculation

The Absorption Cross Section. The polarization of the absorption cross section can be described in terms of 2×2 density matrices such as:

$$\begin{pmatrix} \rho_{11}^{ij} & \rho_{12}^{ij} \\ \rho_{21}^{ij} & \rho_{22}^{ij} \end{pmatrix}$$

where sites are labeled by j and the hyperfine components of a resonance by i.[7] The normalization conditions are $\sum_i \rho_{11}^{ij} = \sum_i \rho_{22}^{ij} = 1$ and $\sum_i \rho_{12}^{ij} = \sum_i \rho_{21}^{ij} = 0$. The density matrix can always be diagonalized if the direction of observation is in a mirror or glide plane, along a 3-fold or higher rotation or a screw axis, and normal to a suitable 2-, 4-, 6-fold rotation axis. Furthermore, if there is only one resonant site per unit cell, then the density matrix can always be diagonalized for any observation direction.

$(CH_3)_2SnF_2$ has only one resonant site per unit cell, and $(CH_3)_2SnCl_2$ has three 2-fold rotation axes parallel to the a, b, and c axes. In these single crystals, therefore, the density matrix is diagonalized for the observation direction normal to the a axis.

If there are only two absorption lines in the spectrum, as in the case for the $I=1/2\rightarrow3/2$ nuclear transition, appropriate density matrix elements for a single site, j, have been shown to be:

$$\begin{aligned} \rho_{11}^{j} &= 1/2 \pm (1/4)w(1+\eta\cos2\phi_j) \\ \rho_{22}^{j} &= 1/2 \pm (1/4)w(1-3\sin^2\theta_j-\eta\cos^2\theta_j\cos2\phi_j) \\ \rho_{12}^{j} &= \rho_{21}^{j} = \pm(\eta/4)w\cos\theta_j\sin2\phi_j \end{aligned} \quad (1)$$

where $w=[3/(3+\eta^2)]^{1/2}$, where the upper signs correspond to the $\pm1/2\rightarrow\pm3/2$ (π) transitions and the lower to the $\pm1/2\rightarrow\pm1/2$ (σ) transitions, and where θ_j and ϕ_j are polar angles with respect to the principal-axes system (PAS) of the EFG.

Let us transform Relation (1) from the θ_j and ϕ_j coordinates to the Θ and Φ coordinates, which define the crystal axes with respect to the incident radiation beams, as is illustrated in Fig. 2. Since the $\boldsymbol{a}$, $\boldsymbol{b}$, and $\boldsymbol{c}$ directions are orthogonal with one another, the following expressions relate θ_j, ϕ_j to Θ, Φ, and the Euler angles $(\alpha_j, \beta_j, \gamma_j)$ which relate the j site to the axes $(\boldsymbol{a}, \boldsymbol{b}, \boldsymbol{c})$:

$$\begin{aligned} \sin\theta_j\cos\phi_j &= \sin\Theta\cos\Phi(\boldsymbol{b}\cdot\boldsymbol{x}_j) + \sin\Theta\sin\Phi(\boldsymbol{c}\cdot\boldsymbol{x}_j) \\ &\quad + \cos\Theta(\boldsymbol{a}\cdot\boldsymbol{x}_j) \equiv B_j \\ \sin\theta_j\sin\phi_j &= \sin\Theta\cos\Phi(\boldsymbol{b}\cdot\boldsymbol{y}_j) + \sin\Theta\sin\Phi(\boldsymbol{c}\cdot\boldsymbol{y}_j) \\ &\quad + \cos\Theta(\boldsymbol{a}\cdot\boldsymbol{y}_j) \equiv C_j \\ \cos\theta_j &= \sin\Theta\cos\Phi(\boldsymbol{b}\cdot\boldsymbol{z}_j) + \sin\Theta\sin\Phi(\boldsymbol{c}\cdot\boldsymbol{z}_j) \\ &\quad + \cos\Theta(\boldsymbol{a}\cdot\boldsymbol{z}_j) \equiv A_j \end{aligned} \quad (2)$$

where:

$$\begin{aligned} (\boldsymbol{b}\cdot\boldsymbol{x}_j) &= \cos\alpha_j\cos\beta_j\cos\gamma_j - \sin\alpha_j\sin\gamma_j \\ (\boldsymbol{c}\cdot\boldsymbol{x}_j) &= -\cos\alpha_j\cos\beta_j\sin\gamma_j - \sin\alpha_j\cos\gamma_j \\ (\boldsymbol{a}\cdot\boldsymbol{x}_j) &= \cos\alpha_j\sin\beta_j \\ (\boldsymbol{b}\cdot\boldsymbol{y}_j) &= \sin\alpha_j\cos\beta_j\cos\gamma_j + \cos\alpha_j\sin\gamma_j \\ (\boldsymbol{c}\cdot\boldsymbol{y}_j) &= -\sin\alpha_j\cos\beta_j\sin\gamma_j + \cos\alpha_j\cos\gamma_j \\ (\boldsymbol{a}\cdot\boldsymbol{y}_j) &= \sin\beta_j\sin\gamma_j \\ (\boldsymbol{b}\cdot\boldsymbol{z}_j) &= -\sin\beta_j\cos\gamma_j \\ (\boldsymbol{c}\cdot\boldsymbol{z}_j) &= \sin\beta_j\sin\gamma_j \\ (\boldsymbol{a}\cdot\boldsymbol{z}_j) &= \cos\beta_j \end{aligned} \quad (3)$$

From Eq. 2, it may be shown that Eq. 1 has the form of:

$$\begin{aligned} \rho_{11}^{j} &= 1/2 \pm (1/4)w\{1+\eta(B_j^2-C_j^2)/(1-A_j^2)\} \\ \rho_{22}^{j} &= 1/2 \pm (1/4)w\{1-3(1-A_j^2) \\ &\quad -\eta A_j^2(B_j^2-C_j^2)/(1-A_j^2)\} \\ \rho_{12}^{j} &= \rho_{21}^{j} = \mp(\eta/2)wA_jB_jC_j/(1-A_j^2) \end{aligned} \quad (4)$$

Absorption Areas. Since the ^{119}Sn first excited state has a spin of 3/2, as a result of the interaction of the nuclear quadrupole moment with the EFG, the resonance absorption line splits into two components, whose separation is given by:

$$\Delta E = (1/2)e^2qQ(1+\eta^2/3)^{1/2} \quad (5)$$

where eq is the EFG in the z (major-axis) direction, η the asymmetry about the z axis ($0\leq\eta<1$) and eQ the nuclear quadrupole moment of the first excited state of ^{119}Sn.

If the observed spectrum has the form of the individual, completely split components—*i.e.*, if the energy difference between components is larger than the absorption line width, then the absorption area, A_i, for the i-th component of the spectrum of the absorber with the effective cross section of T_a is given by:

$$A_i = \alpha f\pi K(T_{ia}) \quad (6)$$

where:

$$\begin{aligned} K(T_{ia}) &= T_{ia}\exp(-T_{ia}/2)[I_0(T_{ia}/2)+I_1(T_{ia}/2)], \\ T_{ia} &= b_iT_a, \end{aligned}$$

α is the fraction of the resonance quanta in the emission spectrum; f, the recoilless fraction of the source, $I_0(x)$ and $I_1(x)$, the zero- and the first-order Bessel function and imaginary argument respectively, and b_i, the relative intensity of the i-th component.[14] If we are considering a polarized absorber (such as a single crystal) with two independent polarizations of the cross section, ρ_{11}^{i} and ρ_{22}^{i}, then the area of the i-th component

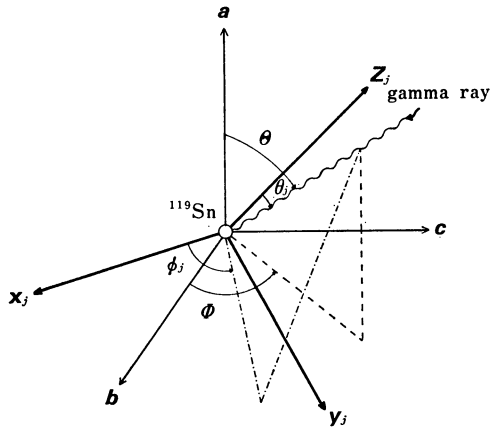

Fig. 2. The orientation of the incident radiation beam relative to the crystal axes (**a**, **b**, **c**) and the EFG axes ($\mathbf{x}_j$, $\mathbf{y}_j$, $\mathbf{z}_j$) of the j-th site in the unit cell.

is given by[8]:

$$A_i = \alpha f\pi[(1/2)K(\rho_{11}^i T_a)+(1/2)K(\rho_{22}^i T_a)] \quad (7)$$

Density Matrix for Two Sites in $(CH_3)_2SnCl_2$. If we let $\boldsymbol{k}_j$ stand for either $\boldsymbol{x}_j$, $\boldsymbol{y}_j$, or $\boldsymbol{z}_j$, the symmetry relation between two sites in the unit cell is a 180° rotation about the a axis and can be written as:

$$\begin{aligned}(\boldsymbol{b}\cdot\boldsymbol{k}_1) &= -(\boldsymbol{b}\cdot\boldsymbol{k}_2)\\ (\boldsymbol{c}\cdot\boldsymbol{k}_1) &= -(\boldsymbol{c}\cdot\boldsymbol{k}_2)\\ (\boldsymbol{a}\cdot\boldsymbol{k}_1) &= (\boldsymbol{a}\cdot\boldsymbol{k}_2)\end{aligned} \quad (8)$$

Consequently, from Eqs. 2 and 8, for observation in the bc plane, *i.e.*, for $\Theta=90°$, the diagonal elements of the density matrix are the same for both sites. The resulting diagonal elements of the density matrix are:

$$\begin{aligned}\rho_{11} &= (1/2) \pm (1/4)w\{1+\eta(B'^2-C'^2)/(1-A'^2)\}\\ \rho_{22} &= (1/2) \pm (1/4)w\{1-3(1-A'^2)\\ &\quad -\eta A'^2(B'^2-C'^2)/(1-A'^2)\}\end{aligned} \quad (9)$$

where:

$$\begin{aligned}A' &= \cos\Phi(\boldsymbol{b}\cdot\boldsymbol{z}) + \sin\Phi(\boldsymbol{c}\cdot\boldsymbol{z})\\ B' &= \cos\Phi(\boldsymbol{b}\cdot\boldsymbol{x}) + \sin\Phi(\boldsymbol{c}\cdot\boldsymbol{x})\\ C' &= \cos\Phi(\boldsymbol{b}\cdot\boldsymbol{y}) + \sin\Phi(\boldsymbol{c}\cdot\boldsymbol{y})\end{aligned}$$

Eq. 9 also holds for observation along the a axis; *i.e.*, $\Theta=0°$, where:

$$A' = (\boldsymbol{a}\cdot\boldsymbol{z}), \quad B' = (\boldsymbol{a}\cdot\boldsymbol{x}), \quad C' = (\boldsymbol{a}\cdot\boldsymbol{y})$$

Note that these equations are ill-conditioned if $1-A'^2=0$; *i.e.*, $\beta=90°$ and $\alpha=\Phi$ in the first case, and $\beta=0°$ in the second.

Recoilless Fraction. When the recoilless fraction of the absorber is f', the effective cross section can be written as $T_a=nf'\sigma_0$, where n is the number of resonant nuclides per cm², and σ_0, a resonant cross section. Therefore, the effective cross section, T_a, depends on f'.

From the elementary theory of the Mössbauer-Lamb fraction, the dependence of the recoilless fraction on the mean-square amplitude of the vibration ($\langle u^2\rangle$) is given by:

$$f' = \exp(-\langle u^2\rangle/\lambda\!\!\!^{-2}) \quad (10)$$

where $2\pi\lambda\!\!\!^{-}=hc/E$, the gamma quatum wavelength, which for ^{119}Sn is 5.190×10^{-9} cm. For an axial-symmetric crystal, using the model for the angular distribution of MSD given by Kündig *et al.*,[15]

$$\langle u^2\rangle(\theta') = \langle u_\perp{}^2\rangle \sin^2\theta' + \langle u_{//}{}^2\rangle \cos^2\theta' \quad (11)$$

where $\langle u_\perp{}^2\rangle$ and $\langle u_{//}{}^2\rangle$ are components of the MSD tensor normal to and parallel to its principal axis, and θ', the polar angle made by the gamma-ray-propagation vector, $\boldsymbol{k}$, with respect to the PAS of the MSD tensor. From Eqs. 10 and 11, the recoilless fraction for the powder sample is given by:

$$f' = \exp\{-(1\lambda\!\!\!^{-}/^2)(\langle u_{//}{}^2\rangle+2\langle u_\perp{}^2\rangle)/3\} \quad (12)$$

By assuming a Debye model for the phonon spectrum, the temperature dependence of the recoilless fraction is given by the well-known expression[16]:

$$f' = \exp\{-(3E_R/2k\theta_D)[1+4(T/\theta_D)^2\int_0^{\theta_D/T} xdx/(e^x-1)]\} \quad (13)$$

in which, within the high-temperature limit, ($T\geq\theta_D/2$) takes the form of:

$$f' = \exp[(-6E_R/k\theta_D{}^2)T] \quad (14)$$

where E_R is the recoil energy of the free nucleus, and θ_D, the Debye temperature. Therefore, if the MSD or the Debye temperature is known, f' can be estimated from Eqs. 10, 12, and 13.

From Eq. 6, if a second spectrum is determined using a similar absorber k times as thick as the original one, the ratio of the intensity is determined as follows:

$$A_i'/A_i = K(kb_inf'\sigma_0)/K(b_inf'\sigma_0) \quad (15)$$

where $k=n'/n$.

Since A_i', A_i, n', and n are measurable, and since $K(x)$ is assumed to be a Lorentzian, the value of f' can be determined from Eq. 15.

Results and Discussion

$(CH_3)_2SnF_2$. The Mössbauer spectra were obtained at 135K for the single-crystal absorber mounted on the a axis normal to the observation axis. Figure 3 shows two typical experimental spectra. The upper spectrum is observed when the angle of the source radiation is 10° from the c axis of the crystal and the crystal thickness is 29.5 mg/cm² for Sn; the lower spectrum is observed when the direction of the radiation is 45° from the c axis and the crystal thickness is 41.0 mg/cm² for Sn.

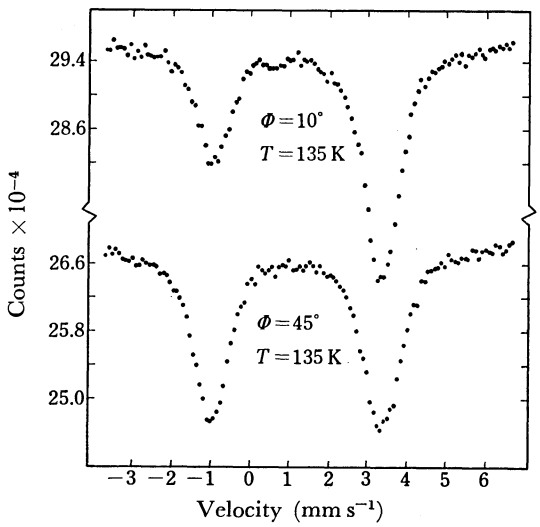

Fig. 3. The Mössbauer absorption spectra of $(CH_3)_2$-SnF_2 single crystal absorber with the direction of observation normal to the a axis.

The room-temperature mean-square amplitude of vibration along the a axis, $\langle u_\perp{}^2\rangle$, and that along the c axis, $\langle u_{//}{}^2\rangle$, have been reported to be 0.0188 Å² and 0.0440 Å² respectively.[11] These values were substituted into Eq. 12 in order to estimate the value of f' at room temperature. Using this value of f', it was estimated from Eq. 14 that the Debye temperature, θ_D, is 115.7 K and that f' is 0.17 at 135 K.

Previously it was mentioned that the tin is surrounded by a octahedron composed of four fluorine atoms and two methyl groups. It will be noted that the C–Sn–C bond direction is assuredly a 4-fold axis, because the angles between the axes of the octahedron are 90°. Therefore, the Sn–C direction is taken as the z axis of the EFG, and the Sn–F(1) and Sn–F(2) directions, as the x and y axis respectively. The EFG is thus axially

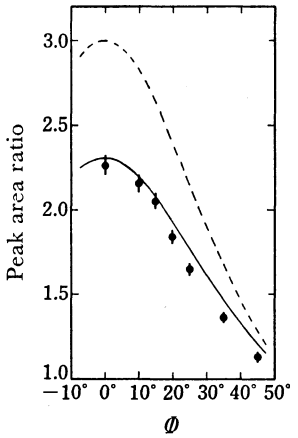

Fig. 4. The area ratio as a function of the observation angle Φ for $(CH_3)_2SnF_2$ single crystal at 135 K. The solid line is computed for $e^2qQ>0$, $\eta=0$, $f'=0.17$, $\alpha=0°$, $\beta=90°$, and $\gamma=90°$. The broken line is computed for neglecting polarization effects.

symmetric ($\eta=0$). Assuming that f' is isotropic, we calculated the area ratio, A_π/A_σ, as a function of the observation angle, Φ, in the bc plane using Eqs. 2, 3, 4, and 7. The assumption that f' is isotropic is supported by the work of Herber and Chandra,[17] who reported that the mean-square amplitudes of vibration of the tin atoms in $(CH_3)_2SnF_2$ were the same in all directions at 140K. The results are shown in Fig. 4. The solid line is the curve computed for $f'=0.17$, $\eta=0$, $\alpha=0°$, $\beta=90°$, and $\gamma=90°$. The broken curve is the line calculated neglecting the effects of polarization, as in Zory.[1] The agreement between the experimental and theoretical results means that the ratio of the high-energy experimental absorption area to the low energy one, A_H/A_L, is equal to A_π/A_σ and not A_σ/A_π. This implies that the $\pm3/2\rightarrow\pm1/2$ transition is higher in energy than the $\pm1/2\rightarrow\pm1/2$ transition, *i.e.*, the sign of the quadrupole interaction (e^2qQ) is positive, which is in accordance with the result obtained by the application of a large external magnetic field.[18]

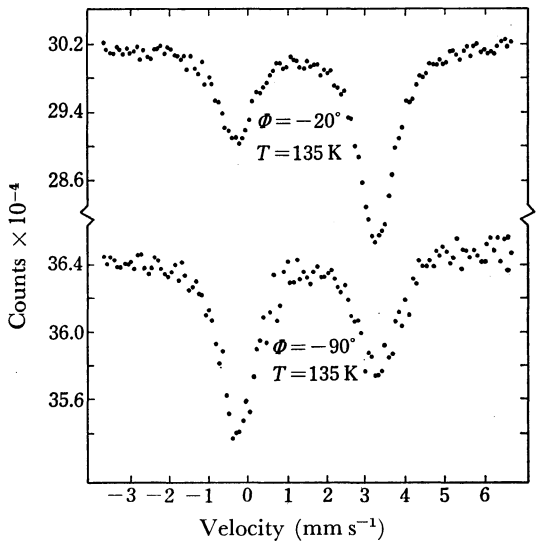

Fig. 5. The Mössbauer absorption spectra of $(CH_3)_2SnCl_2$ single crystal absorber with the direction of observation normal to the a axis.

$(CH_3)_2SnCl_2$. The single-crystal Mössbauer spectra were obtained at 135 K for gamma radiation in the bc plane. The spectra which were obtained for two cases are shown in Fig. 5. In the first case, the gamma ray direction from the b axis was −20° and the thickness was 19.2 mg/cm^2 for Sn, whereas in the second the values are −90° and 28.0 mg/cm^2 respectively.

An approximate value of f' was obtained by the area-ratio method using the powder sample at 100 K. Figure 6 illustrates the results. The low-energy experimental-absorption-area ratios $(A'/A)_L$, are plotted against n'/n. A reasonable fit to the data is obtained for $nf_L'\sigma_0=0.60$, which gives $f'_L=0.10$. A similar analysis for the high-energy experimental-absorption-area ratios $(A'/A)_H$ yields $f'_H=0.11$. Therefore, $f'_L+f'_H=0.21$ is obtained as the recoilless fraction of $(CH_3)_2SnCl_2$ at 100K. Substituting $f'=0.21$ into Eq. 14, the Debye temperature θ_D

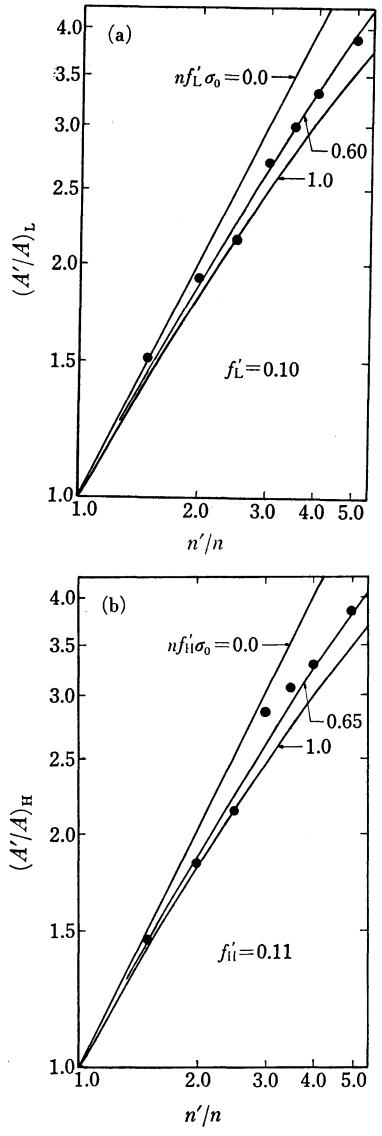

Fig. 6. The absorption area ratio against $(CH_3)_2SnCl_2$ powder absorber thickness ratio at 100 K. (a) The lower energy experimental area ratio $(A'/A)_L$ is plotted against n'/n. (b) The higher energy experimental area ratio $(A'/A)_H$ is plotted against n'/n.

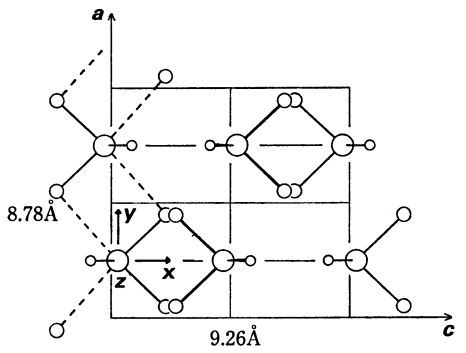

Fig. 7. Projection of the unit cell of $(CH_3)_2SnCl_2$ on the ac plane. ○: Sn, ○: Cl, and ○: C.

is derived as 107.1 K, which is in good agreement with the literature value,[19] 108.3 K at 70 K. Using this value of θ_D, the value of f' at 135 K is found to be nearly equal to 0.12.

In the following discussion, we shall refer only to one site because the two sites are related by a 180° rotation about the a axis. The projection onto the crystallographic ac plane of the unit cell of $(CH_3)_2SnCl_2$ is shown in Fig. 7. Since the tin atom in the unit cell lies on the mirror plane parallel to the ac and bc plane and has C_{2v} symmetry, it can be expected that the principal axes of the EFG tensor lie parallel to the crystallographic a, b, and c axes. However, it is unclear which principal axes of the EFG the a, b, and c axes correspond to; furthermore, the value of η can not be determined from the point symmetry of the tin site itself. Erickson has reported that the sign of V_{zz} in $(CH_3)_2SnCl_2$ is negative.[20] The negative sign of V_{zz} (which corresponds to an excess of the negative charge along the z axis) in *trans*-R_2SnX_4 compounds can most logically be interpreted by assuming that tin-carbon bonds have a much larger p-electron density along the bond that do tin-halogen bonds along their bond axes. Therefore, it seems most likely that the V_{zz} direction is along the b axis.

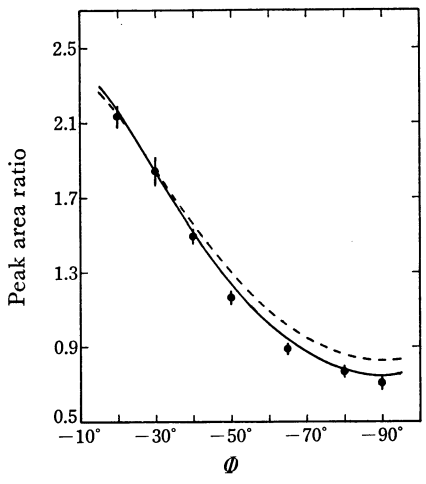

Fig. 8. The area ratio as a function of the observation angle Φ for $(CH_3)_2SnCl_2$ single crystal at 135 K. The dotted curve is computed for $\eta=0.6$, and solid curve for $\eta=0.4$, when $e^2qQ>0, f'=0.12$, $\alpha=0°$, $\beta=90°$, and $\gamma=90°$.

Equations 3, 7, and 9 were evaluated by means of a small computer program to give the density matrix elements for various values of α, β, γ, and η. We assumed that f' was approximately isotropic and that V_{xx} and V_{yy} were parallel to the crystallographic c axis and a axis respectively. The observation angle (Φ) curve for the area ratio was then found using Eq. 7. The results of $\eta=0.4$ and 0.6 are shown, along with the experimental values, in Fig. 8. The dotted curve is computed for $\eta=0.6$, and the solid curve, for $\eta=0.4$, when $f'=0.12$, $\alpha=0°$, $\beta=90°$, and $\gamma=90°$. The agreement between the experimental and calculated values is better when $\eta=0.4$ is used than when $\eta=0.6$ is used. The latter value, which was published previously,[20] must be overestimated. A more detailed value for η may be obtained by comparison with the results of other observations normal to the b axis or the c axis. As we have seen, the thickness of the sample has so profound an effect on the absorption spectra that precise area measurements are necessary to determine the value of η as well as e^2qQ.

We wish to express our sincere gratitude to Assistant Professors Toshihiko Kushi of Hiroshima University and Mitsuo Mishima of Shimane University for their valuable advice in analyzing the data.

References

1) P. Zory, *Phys. Rev.*, **140**, A1401 (1965).
2) J. Danon and L. Iannabrella, *J. Chem. Phys.*, **47**, 382 (1967).
3) K. Chandra and S. P. Puri, *Phys. Rev.*, **162**, 272 (1968).
4) V. K. Garg and S. P. Puri, *J. Chem. Phys.*, **54**, 209 (1971).
5) J. F. Duncan and J. H. Johnston, *Aust. J. Chem.*, **26**, 231 (1973).
6) G. Langonche, M. Van Rossum, K. P. Schmidt, and R. Coussement, *Phys. Rev.*, *B*, **9**, 848 (1974).
7) R. M. Housley, R. W. Grant, and U. Gonser, *Phys. Rev.*, **178**, 514 (1969).
8) T. C. Gibb, *J. Phys. C*, **7**, 1001 (1974).
9) T. C. Gibb, R. Greatrex, and N. N. Greenwood, *J. Chem. Soc., Dalton Trans.*, **1971**, 238.
10) E. O. Schlemper and W. C. Hamilton, *Inorg. Chem.*, **5**, 995 (1966).
11) H. A. Szymwski, "Raman Spectroscopy," Plenum Press, New York (1967), Chap. IV.
12) M. E. Buckley, "Crystal Growth," John Wiley and Sons, New York (1951), p. 35.
13) A. G. Davies, H. J. Milledge, D. C. Puxley, and P. J. Smith, *J. Chem. Soc., A*, **1970**, 2862.
14) G. A. Bykov and Pham zuy Hien, *Sov. Phys.-JETP.*, **16**, 646 (1963).
15) W. Kündig, K. Ando, and H. Bömmel, *Phys. Rev.*, **139**, A889 (1965).
16) V. I. Gol'danskii and R. H. Herber, "Chemical Applications of Mössbauer Spectroscopy," Academic Press, New York (1968), p. 34.
17) R. H. Herber and S. Chandra, *J. Chem. Phys.*, **52**, 6045 (1970).
18) B. A. Goodman and N. N. Greenwood, *J. Chem. Soc., A*, **1971**, 1862.
19) H. A. Stöckler and H. Sano, *Chem. Commun.*, **1969**, 954.
20) N. E. Erickson, *Chem. Commun.*, **1970**, 1349.